

1 **Inferring causal genes at type 2 diabetes GWAS loci through chromosome**
2 **interactions in islet cells**

3

4 **Authors**

5 Jason M. Torres^{1,6,*}, Han Sun², Vibe Nylander³, Damien J. Downes⁴, Martijn van de Bunt^{1,3,7},

6 Mark I. McCarthy^{1,3,8}, Jim R. Hughes^{4,5}, Anna L. Gloyn^{1,2,3}

7 **Affiliations**

8 ¹Wellcome Centre for Human Genetics, University of Oxford, Oxford, UK.

9 ²Department of Pediatrics, Division of Endocrinology and Diabetes, Stanford University
10 School of Medicine, Stanford, CA 94305, USA.

11 ³Oxford Centre for Diabetes Endocrinology & Metabolism, University of Oxford, UK.

12 ⁴Medical Research Council Molecular Haematology Unit, Medical Research Council
13 Weatherall Institute of Molecular Medicine, Radcliffe Department of Medicine, University of
14 Oxford, Oxford, UK.

15 ⁵MRC WIMM Centre for Computational Biology, MRC Weatherall Institute of Molecular
16 Medicine, Radcliffe Department of Medicine, University of Oxford, Oxford, UK.

17 ⁶Present address: Clinical Trial Service Unit and Epidemiological Studies Unit, Oxford
18 Population Health, University of Oxford, OX3 7LF, UK.

19 ⁷Present address: Cytoki Pharma ApS, Tuborg Boulevard 12, DK-2900 Hellerup, DK.

20 ⁸Present address: OMNI Human Genetics, Genentech, 1 DNA Way, South San Francisco, CA
21 94080, USA.

22 * Address for Correspondence: jason.torres@ndph.ox.ac.uk (J.M.T.)

23

24 **Summary**

25 Resolving causal genes for type 2 diabetes at loci implicated by genome-wide association
26 studies (GWAS) requires integrating functional genomic data from relevant cell types.
27 Chromatin features in endocrine cells of the pancreatic islet are particularly informative and
28 recent studies leveraging chromosome conformation capture (3C) with Hi-C based methods
29 have elucidated regulatory mechanisms in human islets. However, these genome-wide
30 approaches are less sensitive and afford lower resolution than methods that target specific
31 loci. To gauge the extent to which targeted 3C further resolves chromatin-mediated
32 regulatory mechanisms at GWAS loci, we generated interaction profiles at 23 loci using next-
33 generation (NG) Capture-C in a human beta cell model (EndoC- β H1) and contrasted these
34 maps with Hi-C maps in EndoC- β H1 cells and human islets and a promoter capture Hi-C
35 map in human islets. We found improvements in assay sensitivity of up to 33-fold and
36 resolved 4.8X more chromatin interactions. At a subset of 18 loci with 25 co-localised
37 GWAS and eQTL signals, NG Capture-C interactions implicated effector transcripts at five
38 additional genetic signals relative to promoter capture Hi-C through physical contact with
39 gene promoters. Therefore, high resolution chromatin interaction profiles at selectively
40 targeted loci can complement genome- and promoter-wide maps.

41

42 **Introduction**

43 Most variants implicated by genome-wide association studies (GWAS) are non-coding and
44 are thought to influence type 2 diabetes risk through regulatory effects on gene expression
45 within physiologically relevant cell types. As such, the process of elucidating causal genes
46 (and their corresponding *effector* transcripts) requires integration of functional genomic and
47 molecular epigenomic information in disease relevant cell types and under relevant
48 conditions. Importantly, regulatory effects on gene expression are facilitated by chromatin
49 interactions and causal genes may be identified by their physical contact with enhancer
50 elements encompassing diabetes-associated variants.

51

52 Recent studies have employed methods based on chromatin conformation capture (3C) and
53 implicated genes at GWAS loci associated with type 2 diabetes by mapping chromatin
54 structure in human islets and beta cells (Greenwald et al., 2019; Lawlor et al., 2019; Miguel-
55 Escalada et al., 2019; Su et al., 2022). All 3C protocols involve the same core key steps –
56 fixation of chromatin with formaldehyde, restriction enzyme digestion, and re-ligation of
57 restriction fragments (Davies et al., 2017). The resulting “ligation junctions”, which comprise
58 fragments that are co-localised spatially but may be separated linearly by tens to hundreds of
59 kilobases, are sequenced and incorporated into maps of interacting chromatin. Variations in
60 preparing the 3C library and extracting ligation junctions of interest can influence the
61 resolution, sensitivity, and genomic coverage of the resulting chromatin maps, therefore the
62 choice of 3C-based method can markedly alter the detail of chromatin structure information.
63 These differences may affect the inferences made about islet cell biology and the role of T2D
64 associated GWAS variants.

65

66 To date, 3C maps in human islets and beta cells have been based on Hi-C approaches that
67 provide genome-wide coverage (and can be enriched for ligation junctions involving
68 promoters), but afford limited detail at individual loci due to prohibitive sequencing
69 requirements and use of low-resolution restriction enzymes (Davies et al., 2017).
70 Alternatively, the NG Capture-C method enables improved resolution and sensitivity at target
71 loci, also referred to as viewpoints or baits, through enrichment from high-resolution 3C
72 libraries (Davies et al., 2017; Hughes et al., 2014).

73 To assess the extent to which chromatin maps generated from different 3C-based methods
74 impact mechanistic inference at T2D GWAS loci, we performed a systematic evaluation of
75 27 gene promoters at 23 loci. We performed *next generation* (NG) Capture-C, which involves
76 a double capture procedure that can enrich for captured fragments by up to 1,000,000-fold
77 (Davies et al., 2015), and targeted promoters in the EndoC- β H1 human beta cell line
78 (Ravassard et al., 2011). We also mapped chromatin interactions using sequenced ligation
79 junctions from recent studies that applied Hi-C in EndoC- β H1 cells and human islets, and
80 promoter-capture (pc) Hi-C in human islets (Lawlor et al., 2019; Miguel-Escalada et al.,
81 2019). By comparing these maps with those from NG Capture-C and incorporating GWAS
82 variants co-localised with expression quantitative trait loci (eQTLs) in human islets, we show
83 how distinct chromatin profiles influence the resolution of causal genes for T2D and
84 glycaemic traits.

85

86 **Results**

87 We compared chromatin interaction maps for 27 promoters at 23 loci in human EndoC- β H1
88 cells, derived from NG Capture-C, with previously published Hi-C maps (Lawlor et al.,
89 2019) in EndoC- β H1 cells and human islets, and with a pcHi-C map (Miguel-Escalada et al.,
90 2019) in human islets. These experiments showed marked differences in sensitivity with the
91 NG Capture-C EndoC- β H1 experiment yielding up to ~ 27 X more ligation junctions than the
92 Hi-C based studies (**Supplemental Table 2**). We assessed how these experimental
93 differences impacted our ability to resolve chromatin interactions. We applied a Bayesian
94 model implemented in peaky (Eijsbouts et al., 2019) to detect fragments showing significant
95 physical interaction with each of the viewpoint (a.k.a. “bait”) fragments encompassing the
96 targeted promoters. Due to the sparsity of per-fragment ligation junction reads, the peaky
97 algorithm failed to converge (and hence unable to perform statistical tests) for six viewpoints
98 in the pcHi-C islet dataset and for all 27 viewpoints in the Hi-C datasets (**Supplemental**
99 **Table 3**). In contrast, peaky successfully mapped interactions at all viewpoints in the NG
100 capture-C EndoC- β H1 experiment. After merging adjacent fragments with significant
101 interactions, there were 3.6X as many interactions identified by peaky for NG Capture-C than
102 for pcHi-C. Moreover, the median width of significantly interacting chromatin regions was
103 14.3-fold shorter, indicating a greater ability to fine-map interactions in addition to increased
104 sensitivity (**Supplemental Table 3**).

105 We also found that interaction peaks resolved by the NG Capture-C experiment were more
106 significantly enriched for islet regulatory features than those gleaned from the pcHi-C
107 experiment (**Supplemental Figure 1**). Enriched islet features included accessible chromatin
108 peaks (Fisher’s exact test odds ratio [OR]=2.17, 95% CI [1.95, 2.40]), H3K27ac ChIP-seq
109 peaks (OR=2.66, 95% CI [2.43, 2.91]) and active promoter (OR=2.85, 95% CI [2.34, 3.45])
110 and enhancer elements (e.g. type 1 active enhancer, OR=2.07, 95% CI [1.72, 2.46]).

111 To assess how different chromatin interaction profiles impact mechanistic inference at
112 GWAS loci, we integrated single nucleotide polymorphisms (SNPs) associated with islet
113 gene expression (i.e. eSNPs) and type 2 diabetes and/or glycaemic traits. Of the 27 captured
114 promoters, 21 corresponded to eGenes implicated at 18 loci by 25 pairs of co-localised eSNP
115 and GWAS variants (**Supplemental Table 1**). A total of 12 of these co-localised signals were
116 supported by either NG Capture-C (n=10) or pcHi-C (n=7), with five receiving support from
117 both methods (**Supplemental Table 4**). Included in this set of five was a signal at the
118 *CAMK1D* locus where a genetic association with type 2 diabetes involving SNP rs11257655
119 is co-localised with an eQTL involving rs11257658 (linkage disequilibrium $r^2=0.994$). The G
120 allele of rs11257658 is associated with decreased human islet expression of *CAMK1D* which
121 encodes calcium/calmodulin-dependent protein kinase 1D (van de Bunt et al., 2015; Viñuela
122 et al., 2020). Both variants, located ~82 kb upstream of the *CAMK1D* promoter, map to
123 chromatin that physically interacts with the promoter site, thereby corroborating the eQTL
124 (**Figure 1A**). Although the resolution in the pc-HiC study was markedly lower than that for
125 capture-C, the interaction maps from both experiments support *CAMK1D* as the effector gene
126 at this locus.

127 Furthermore, there were five genetic signals supported by chromatin interactions only in our
128 NG Capture-C experiment. This included a co-localised eQTL-GWAS signal fine-mapped to
129 a single SNP (rs11708067) at the *ADCY5* locus where the A allele associates with lower islet
130 expression of *ADCY5*, greater T2D risk, and higher levels of fasting glucose (van de Bunt et
131 al., 2015; Dupuis et al., 2010; Morris et al., 2012; Viñuela et al., 2020; Voight et al., 2010)
132 (**Figure 1B**). We previously reported a chromatin interaction at this locus and allelic
133 imbalance where the risk A allele at rs11708067 associated with decreased chromatin
134 accessibility (Turner et al., 2018). Another notable example occurred at the *DGKB* locus
135 where there are two independent T2D-associated signals: rs10228066 and rs17168486.

136 Whereas no significant chromatin interactions were detectable at this locus in the pcHi-C and
137 Hi-C experiments due to low signal, multiple interaction peaks were resolved from the NG
138 Capture-C data, including peaks near the T2D-associated SNPs. The rs17168486 variant,
139 located ~45 kb upstream of the *DGKB* promoter, mapped within 500 bp of chromatin that
140 significantly interacts with the *DGKB* promoter region (**Figure 1C**). Notably, this SNP –
141 where the T2D risk allele T associates with increased expression of *DGKB* in human islets
142 (Viñuela et al., 2020) – also overlaps enhancer elements in islets and EndoC-βH1 cells (but
143 not in liver, adipose, or skeletal muscle) and accessible chromatin in primary alpha and beta
144 cells (i.e. single-nucleus ATAC-seq peaks) (**Figure 1D**). Moreover, this chromatin accessible
145 region was recently predicted to regulate the expression of *DGKB* in human beta cells with
146 high-insulin content (Chiou et al., 2021), which is further supported by *in vitro* data
147 demonstrating the T2D risk haplotype at rs17168486 influenced luciferase expression in
148 832/13 and MIN6 cells (Viñuela et al., 2020). In contrast, the rs10228066 variant, located
149 ~121 kb downstream of the *DGKB* promoter and co-localised with the rs10231021 eQTL
150 signal (LD $r^2=0.881$), mapped more than 1.7 kb from the nearest chromatin interaction.
151 Moreover, neither rs10231021 nor rs10228066 directly overlapped accessible chromatin in
152 EndoC-βH1 or islet cell types (**Figure 1E**). Furthermore, in a recent trans-ethnic GWAS
153 meta-analysis involving 180,834 T2D cases and 1.159M controls, the rs17168486 signal was
154 fine-mapped to a single variant (rs17168486) whereas the other conditionally independent
155 signal at the *DGKB* locus (where the lead SNP rs2215383 is in strong linkage disequilibrium
156 with rs10228066; $r^2=0.999$ in the TOPMED European dataset) was less resolved (13 credible
157 variants and credible interval of 2,318 bp) (Mahajan et al., 2020) and had a credible interval
158 that did not overlap or map within 500 bp of a chromatin interaction. However, a T2D risk
159 haplotype involving variants in high LD with the rs10231021 eSNP did show higher

160 luciferase expression in 832/13 and MIN6 cells with three variants also showing allele-
161 specific binding in a mobility shift assay (Viñuela et al., 2020).

162 Despite the higher resolution afforded by the NG Capture-C procedure, there were two
163 genetic signals supported by chromatin interactions only in the pcHi-C experiment in human
164 islets: *TCF7L2* and *UBE2E2* (**Supplemental Table 4**). At the *TCF7L2* locus, which has been
165 fine mapped to a single SNP, rs7903146, the T2D risk allele (T) associates with increased
166 *TCF7L2* expression in islets (Viñuela et al., 2020) and the SNP overlaps an islet enhancer
167 element and accessible chromatin in bulk islet tissue and islet alpha, beta, and delta cells
168 (**Supplemental Figure 2, Supplemental Table 5**). Notably, chromatin accessibility at this
169 region was considerably lower in EndoC-βH1 cells than in islets ($\log_2FC = -2.07$; FDR-
170 adjusted p-value = $1.68e-07$). Therefore, the lower accessibility in this cell-type may explain,
171 in part, the lack of pronounced chromatin interaction at this site from the NG Capture-C
172 profile. In the case of *UBE2E2*, a T2D-associated SNP rs35352848 is co-localised with an
173 eQTL (rs13094957) for *UBE2E2* expression in islets and overlapped a broad islet pcHi-C
174 chromatin interaction with the *UBE2E2* promoter. However, neither variant directly maps to
175 H3K27ac peaks, enhancer elements, or accessible chromatin in islets, or in snATAC-seq
176 peaks in beta, alpha, or delta cells (**Supplemental Table 5**). Notably, a recent trans-ancestry
177 GWAS meta-analysis fine-mapped this signal to six credible variants and a wide credible
178 interval of nearly 200 kb (overlapping 12 chromatin interactions). Therefore, more
179 investigation is needed to resolve the causal variant at this signal.

180

181 **Discussion**

182 We found that NG Capture-C achieved substantially greater resolution and sensitivity over
183 Hi-C based approaches at the loci we investigated in human beta cells. This corresponded to
184 enhanced fine-mapping of chromatin interactions that were more enriched for accessible
185 chromatin peaks and islet regulatory elements than interactions gleaned from the pcHi-C
186 experiment. Chromatin interactions provided support for genes implicated by GWAS and
187 eQTL co-localization at 12 of 25 evaluated signals, with five signals supported by
188 interactions in the both the pcHi-C and NG Capture-C experiments. Relative to the pcHi-C
189 study, interactions from our NG Capture-C study corroborated five additional target genes:
190 *ADCY5*, *DGKB*, and three genes at the *GPSM1* locus (*DNLZ*, *CARD9*, and *GPSM1*).
191 Experimental studies have implicated both *ADCY5* and *DGKB* in insulin secretion, with
192 *ADCY5* shown to be indispensable for glucose-induced insulin secretion in human islets
193 (Hodson et al., 2014; Peiris et al., 2018). Furthermore, our results corroborate co-localized
194 GWAS and islet eQTL signals at the *GPSM1* locus. Notably, of the signals evaluated in this
195 study, only chromatin encompassing the SNP rs28505901 at this locus showed a significantly
196 stronger interaction in EndoC- β H1 cells relative to LCLs, specifically with the *DNLZ*
197 promoter (**Supplemental Table 4**).

198

199 Chromatin interactions from the EndoC- β H1 NG Capture-C experiment did not corroborate
200 candidate disease genes at all evaluated loci, with *TCF7L2* being the most salient exception.
201 We observed lower chromatin accessibility in EndoC- β H1 cells at this site which may reflect
202 an epigenomic profile corresponding to an earlier developmental stage. Hence, the
203 discrepancy at this locus may be a consequence of EndoC- β H1 cells being a fetal-derived cell
204 line rather than evidence against a mechanism of action in beta cells. Due to the relatively
205 modest number of viewpoints interrogated in this study, it is unclear if such discordances are

206 primarily due to inherent epigenomic differences between cell and tissue types. The
207 unavailability of pcHi-C data in EndoC- β H1 cells and NG Capture-C data in islets also
208 limited our comparisons as we could not control for cell-type in our evaluation of these two
209 approaches. It is possible that interactions detected in islets but not in EndoC- β H1 cells may
210 reflect enhancer-promoter loops specific to other islets cell types. Notably, a recent study of
211 Hi-C maps in FACS sorted islet cells implicated alpha cells at a T2D-associated signal at the
212 *WFS1* locus, and acinar cells at a signal mapping to the *CPA4* locus (Su et al., 2022).
213 Differences in interaction profiles between islets and EndoC- β H1 cells may also reflect
214 distinct epigenomic features resulting from SV40LT transduction. Additional chromatin maps
215 will be needed to fully address these questions and recent improvements in NG Capture-C
216 technology may make application in rarer cell populations more tractable (Downes et al.,
217 2021). However, we have demonstrated that markedly enriching 3C libraries for promoters of
218 interest can reveal additional interactions at type 2 diabetes and glycaemic trait-associated
219 loci. Therefore, selective capture of fine-mapped genetic loci may greatly complement
220 genome- or promoter-wide chromatin maps.

221

222 **Author contributions**

223 J.M.T, V.N, M.I.M, and A.L.G conceived and planned the main analysis. J.M.T. conducted
224 bioinformatic and statistical analysis of the NG Capture-C sequencing data. H.S. performed
225 bioinformatic analyses of the Hi-C and pcHi-C sequencing data. V.N. and D.J.D. cultured
226 EndoC- β H1 and LCL cells and performed the NG Capture-C protocol. M.v.d.B. contributed
227 to the experimental design and selection of loci to target for NG Capture-C. J.R.H. and D.J.D.
228 provided valuable insight into the analysis and interpretation of the NG Capture-C
229 experiment. M.I.M. and A.L.G. supervised this work. J.M.T. wrote the first draft of the

230 manuscript and J.M.T. and A.L.G. edited the manuscript. All authors approved the
231 manuscript.

232

233 **Acknowledgments**

234 A.L.G. is a Wellcome Senior Fellow in Basic Biomedical Science. A.L.G. is funded by the
235 Wellcome (200837) and National Institute of Diabetes and Digestive and Kidney Diseases
236 (NIDDK) (U01-DK105535; U01-DK085545, UM1DK126185). This work was carried out as
237 part of the WIGWAM Consortium (Wellcome Investigation of Genome Wide Association
238 Mechanisms) funded by a Wellcome Trust Strategic Award (106130/Z/14/Z) to M.I.M, J.H
239 and A.L.G. This research was also supported by the Wellcome Trust Core Award Grant
240 Number 203141/Z/16/Z with additional support from the NIHR Oxford BRC. The views
241 expressed are those of the author(s) and not necessarily those of the NHS, the NIHR or the
242 Department of Health.

243

244 **Declaration of Interests**

245 As of June 2019, M.I.M. is an employee of Genentech and a holder of Roche stock. J.R.H. is
246 a founder and shareholder of, and J.R.H. and D.J.D. are paid consultants for Nucleome
247 Therapeutics. J.R.H holds patents for NG Capture-C (WO2017068379A1, EP3365464B1,
248 US10934578B2). ALG's spouse is an employee of Genentech and a holder of Roche stock.

249

250 **STAR Methods**

251 **RESOURCE AVAILABILITY**

252 **Lead contact**

253 Further information and requests for resources and reagents should be directed to and will be
254 fulfilled by the lead contact, Jason Torres (jason.torres@ndph.ox.ac.uk).

255 **Materials availability**

256 This study did not generate new unique reagents.

257 **Data and code availability**

258 NG capture-C sequencing data from EndoC- β H1 cells and LCL cells have been deposited on
259 the European Genome-phenome Archive (EGA), which is hosted by the European
260 Bioinformatics Institute of the European Molecular Biology Laboratory (EMBL-EBI) and the
261 Centre for Genomic Regulation (CRG), under accession number EGAS00001006105 and
262 will be released upon publication. ATAC-seq data from EndoC- β H1 have also been deposited
263 on EGA under accession number EGAS00001006105. Further information about EGA can be
264 found on <https://ega-archive.org>. All original code has been deposited at Zenodo and is
265 publicly available as of the date of publication. DOIs are listed in the key resources table.
266 This paper analyzes existing, publicly available data. Source data and publicly available
267 resources used for this study supporting all findings are detailed in the key resources table.
268 Any additional information required to reanalyze the data reported in this paper is available
269 from the lead contact upon request.

270

271 **EXPERIMENTAL MODEL AND SUBJECT DETAILS**

272 EndoC- β H1 cells (RRID: CVCL_L909) were purchased from Endocell, and cultured as
273 described previously (Hastoy et al., 2018; Ravassard et al., 2011). Lymphoblastoid cell lines
274 (GM12878; RRID: CVCL_7526) were procured from the Coriell Institute. Publicly available
275 *MboI* enzyme-based Hi-C sequencing data corresponding to EndoC- β H1 cells and human
276 islets (n=1), were accessed (Lawlor et al., 2019). Promoter capture Hi-C (pHi-C) data
277 corresponding to human islets from four donors were downloaded from the EGA database
278 (accession EGAS00001002917).

279

280 **METHOD DETAILS**

281

282 *Next Generation Capture-C*

283 Promoters for 27 gene transcripts at 23 loci were selected for capture. These included 21
284 genes at 18 loci harbouring both islet eQTLs and genome-wide significant associations with
285 type 2 diabetes and/or glycaemic traits (van de Bunt et al., 2015; Viñuela et al., 2020). The six
286 remaining genes included three control genes with high expression in lymphoblastoid cell
287 lines (LCLs), the *GCK* gene encoding glucokinase (implicated in monogenic forms of
288 diabetes and hyperinsulinemia), and two genes (*CDKALI* and *SOX4*) at the *CDKALI* locus
289 associated with T2D (**Supplemental Table 1**). 70-mer biotinylated oligonucleotide probes
290 (IDT xGen Lockdown oligonucleotides) targeting *DpnII* restriction fragments were designed
291 using CapSequm (Hughes et al., 2014) with filtering for repetitive elements, duplicates (≤ 2),
292 BLAT density score (≤ 40), and GC content ($\leq 60\%$) (Downes et al., 2022).

293 *In situ* 3C libraries were generated in EndoC- β H1 cells and LCLs by *DpnII* digestion and T7
294 ligation chromatin (Davies et al., 2015); 3C material was sonicated to 200 base pairs (bp) and
295 index using NEB Next DNA library prep reagents. Indexed libraries were pooled and double
296 capture performed with Nimblegen SeqCap EZ reagents (Roche) (Davies et al., 2015).
297 Sequencing was performed on the Illumina NextSeq platform with 150 bp paired-end reads.
298 Sequenced reads were mapped to GRCh38 with bowtie using CCseqBasicS (Telenius et al.,
299 2020) which trims adaptor sequences, reconstructs read pairs with flash, conducts an *in silico*
300 digestion of *DpnII* fragments, maps reads, identifies paired “capture” and “reporter”
301 fragments, and filters PCR duplicates.

302

303 *Hi-C and Promoter capture Hi-C*

304 Hi-C sequencing data for EndoC- β H1 cells and human islets were processed using the Juicer
305 (v1.75) pipeline (Durand et al., 2016). Sequencing reads from the *Hind*III-digested pcHi-C
306 library were processed and mapped to genome build GRCh38 using HiCUP (v0.8.1) (Wingett
307 et al., 2015). Bait and prey fragments were quantified using *chicagoTools* from the
308 CHiCAGO package (v1.14.0) (Cairns et al., 2016). Promoter bait design coordinates for
309 genome build hg19 were obtained from this study (Javierre et al., 2016). and lifted over to
310 GRCh38 using LiftOver.

311

312 *ATAC-seq*

313 ATAC library preparation and sequencing was performed for 11 EndoC- β H1 cell lines using
314 the same protocols used in Thurner et al. 2018 (Thurner et al., 2018). Human islet ATAC
315 sequencing data corresponding to 13 donors from the Miguel-Escalada et al. 2019 study was
316 accessed from the EGA database (accession EGAS00001002917). Sequencing reads were
317 processed and mapped to GRCh38 using the ENCODE ATAC-seq bioinformatic pipeline
318 (v1.9.3), with peak calling performed with MACS2 (v2.7.1) (Feng et al., 2012) using default
319 parameters. Reads within peaks were quantified with *featureCounts* (v2.0.1) (Liao et al.,
320 2019) and normalized by median of observed count ratio *size factors* with DESeq2 (v1.26.0)
321 (Love et al., 2014).

322

323 **QUANTIFICATION AND STATISTICAL ANALYSIS**

324 NG Capture-C reporter counts for each replicate (n=3) of EndoC- β H1 and LCL cells were
325 normalized to the number of *cis* reporter counts (i.e. same chromosome) per 100,000 *cis*
326 reporter reads with CaptureCompare (Telenius et al., 2020). Chromatin interaction mapping
327 in NG Capture-C, pcHi-C, and Hi-C datasets was performed with *peaky* (Eijsbouts et al.,

328 2019) using recommended settings ($\omega = -3.8$). Interactions were considered significant if
329 the marginal posterior probability of contact (MPPC) exceeding 0.01 within a range of 250
330 kb to the viewpoint (i.e. captured fragment) or 0.1 between 250 kb and 1 Mb relative to the
331 viewpoint. Differential chromatin interactions (NG capture-C) between EndoC- β H1 and LCL
332 cells, and differentially accessible (ATAC-seq) peaks between EndoC- β H1 and primary
333 human islet cells were called using DESeq2 (v1.26.0).

334

335

336 **Main figure title and legend**

337 **Figure 1. Chromatin interaction profiles at trait-associated loci.** Co-localised GWAS-
338 eQTL SNPs are shown with ligation junctions obtained from 3C-based experiments at the (A)
339 *CDC123/CAMK1D*, (B) *ADCY5*, and (C) *DGKB* locus. Tracks of significant chromatin
340 interactions and marginal posterior probability of contact (MPPC) values are shown below
341 the EndoC- β H1 capture-C and islet pcHi-C tracks. Red vertical bars indicate SNP
342 coordinates across 3C-based tracks. Gene annotations correspond to GENCODE V38 protein
343 (blue) and RNA (green) encoding genes. Molecular epigenome profile at the *DGKB* locus is
344 shown for SNPs (D) rs17168486 and (E) rs10231021 and rs10228066. Differential
345 accessibility between EndoC- β H1 and human islets was assessed using DESeq2 and FDR-
346 adjusted $-\log_{10}$ p-values and \log_2 fold changes are shown in the dark and light pink,
347 respectively. Select single nuclear ATAC-seq peaks in islet alpha, beta, and delta cells from
348 Chiou et al. 2021 are shown in dark red. Histone post-translational modification ChIP-seq
349 peaks and regulome annotations in human islets from Miguel-Escalada et al. 2019 are shown
350 in dark gold. Grey vertical grey bars indicate SNP coordinates across tracks.

351

352 **Supplemental item titles and legends**

353 **Supplemental Table 1: Description of captured loci.** Genes targeted in the next-generation
354 capture-C experiment, and evaluated in the promoter capture Hi-C and Hi-C experiments, are
355 listed with their corresponding loci, rationale for inclusion, known GWAS associations with
356 T2D and/or glycemetic traits, and expression quantitative trait loci (eQTL) SNPs (i.e. eSNPs)
357 associated with gene expression in primary human islets. GWAS-eQTL colocalization
358 analysis results reported by the Integrated Network for Systematic analysis of Pancreatic Islet
359 RNA Expression (InsPIRE) consortium are also included from Viñuela et al. 2020.

360

361 **Supplemental Table 2: Comparison of ligation junctions across methods.** For each
362 captured gene, the targeted viewpoint fragment encompassing the gene transcription start site
363 (TSS) is indicated along with descriptive statistics corresponding to the mapped ligation
364 junction reads from the next-generation capture-C experiment in EndoC-betaH1 cells,
365 promoter capture Hi-C experiment in human islets from Miguel-Escalada et al. 2019, and Hi-
366 C experiments in EndoC-betaH1 cells and islets from Lawlor et al. 2019. The overlap region
367 indicates if the TSS overlapped the viewpoint fragment directly (i.e. "viewpoint") or mapped
368 within 1kb of the viewpoint fragment (i.e. "exclusion").

369

370 **Supplemental Table 3: Comparison of significant chromatin interactions mapped with**
371 **peaky.** For each captured locus, the number of restriction fragments with marginal posterior
372 probability (MPPC) exceeding 0.01 within 250k of the viewpoint fragment (i.e. proximal
373 interaction) or exceeding 0.10 within 1Mb of the viewpoint fragment (i.e. distal interaction)
374 are shown for the capture-C and pcHi-C experiments. Interaction peaks are delineated by
375 merging adjacent fragments meeting MPPC significance thresholds.

376

377 **Supplemental Table 4: Integration of peaky interactions with GWAS variants and**
378 **eSNPs.** Significant chromatin interactions at restriction fragments encompassing reported
379 T2D and/or glyceimic trait associated SNPs and/or SNPs associated with gene expression in
380 human islets are shown for the next generation capture-C and pcHi-C experiments. GWAS
381 and eSNPs reported to be significantly colocalized in Viñuela et al. 2020 are indicated. For
382 the capture-C experiment, chromatin that interacted more strongly in EndoC-betaH1 cells
383 relative to LCL cells is also indicated.

384

385 **Supplemental Table 5: Single cell accessible chromatin in pancreas at captured loci.**
386 T2D/glyceimic trait associated SNPs and islet eSNPs at evaluated loci overlapping single
387 nuclear ATAC-seq peaks in pancreas cell types reported in Chou et al. 2021 are indicated.

388 **References**

- 389 van de Bunt, M., Manning Fox, J.E., Dai, X., Barrett, A., Grey, C., Li, L., Bennett, A.J.,
390 Johnson, P.R., Rajotte, R.V., Gaulton, K.J., et al. (2015). Transcript Expression Data from
391 Human Islets Links Regulatory Signals from Genome-Wide Association Studies for Type 2
392 Diabetes and Glycemic Traits to Their Downstream Effectors. *PLOS Genet.* *11*, e1005694–
393 e1005694. .
- 394 Cairns, J., Freire-Pritchett, P., Wingett, S.W., Várnai, C., Dimond, A., Plagnol, V., Zerbino,
395 D., Schoenfelder, S., Javierre, B.-M., Osborne, C., et al. (2016). CHiCAGO: robust detection
396 of DNA looping interactions in Capture Hi-C data. *Genome Biol.* *17*, 127.
397 <https://doi.org/10.1186/s13059-016-0992-2>.
- 398 Chiou, J., Zeng, C., Cheng, Z., Han, J.Y., Schlichting, M., Miller, M., Mendez, R., Huang, S.,
399 Wang, J., Sui, Y., et al. (2021). Single-cell chromatin accessibility identifies pancreatic islet
400 cell type– and state-specific regulatory programs of diabetes risk. *Nat. Genet.* *53*, 455–466.
401 <https://doi.org/10.1038/s41588-021-00823-0>.
- 402 Davies, J.O.J., Telenius, J.M., McGowan, S.J., Roberts, N.A., Taylor, S., Higgs, D.R., and
403 Hughes, J.R. (2015). Multiplexed analysis of chromosome conformation at vastly improved
404 sensitivity. *Nat. Methods* *13*, 74–80. <https://doi.org/10.1038/nmeth.3664>.
- 405 Davies, J.O.J., Oudelaar, A.M., Higgs, D.R., and Hughes, J.R. (2017). How best to identify
406 chromosomal interactions: a comparison of approaches. *Nat Meth* *14*, 125–134. .
- 407 Downes, D.J., Beagrie, R.A., Gosden, M.E., Telenius, J., Carpenter, S.J., Nussbaum, L., De
408 Ornellas, S., Sergeant, M., Eijbsbouts, C.Q., Schwessinger, R., et al. (2021). High-resolution
409 targeted 3C interrogation of cis-regulatory element organization at genome-wide scale. *Nat.*
410 *Commun.* *12*, 531. <https://doi.org/10.1038/s41467-020-20809-6>.
- 411 Downes, D.J., Smith, A.L., Karpinska, M.A., Velychko, T., Rue-Albrecht, K., Sims, D.,
412 Milne, T.A., Davies, J.O.J., Oudelaar, A.M., and Hughes, J.R. (2022). Capture-C: a modular
413 and flexible approach for high-resolution chromosome conformation capture. *Nat. Protoc.* *17*,
414 445–475. <https://doi.org/10.1038/s41596-021-00651-w>.
- 415 Dupuis, J., Langenberg, C., Prokopenko, I., Saxena, R., Soranzo, N., Jackson, A., Wheeler,
416 E., Glazer, N., Bouatia-Naji, N., Gloyn, A., et al. (2010). New genetic loci implicated in
417 fasting glucose homeostasis and their impact on type 2 diabetes risk. *Nat. Genet.* *42*, 105–
418 116. .
- 419 Durand, N.C., Shamim, M.S., Machol, I., Rao, S.S.P., Huntley, M.H., Lander, E.S., and
420 Aiden, E.L. (2016). Juicer Provides a One-Click System for Analyzing Loop-Resolution Hi-
421 C Experiments. *Cell Syst.* *3*, 95–98. <https://doi.org/10.1016/j.cels.2016.07.002>.
- 422 Eijbsbouts, C.Q., Burren, O.S., Newcombe, P.J., and Wallace, C. (2019). Fine mapping
423 chromatin contacts in capture Hi-C data. *BMC Genomics* *20*, 77.
424 <https://doi.org/10.1186/s12864-018-5314-5>.
- 425 Feng, J., Liu, T., Qin, B., Zhang, Y., and Liu, X.S. (2012). Identifying ChIP-seq enrichment
426 using MACS. *Nat. Protoc.* *7*, 1728–1740. <https://doi.org/10.1038/nprot.2012.101>.

- 427 Greenwald, W.W., Chiou, J., Yan, J., Qiu, Y., Dai, N., Wang, A., Nariyai, N., Aylward, A.,
428 Han, J.Y., Kadakia, N., et al. (2019). Pancreatic islet chromatin accessibility and
429 conformation reveals distal enhancer networks of type 2 diabetes risk. *Nat. Commun.* *10*,
430 2078–2078. <https://doi.org/10.1038/s41467-019-09975-4>.
- 431 Hastoy, B., Godazgar, M., Clark, A., Nylander, V., Spiliotis, I., van de Bunt, M., Chibalina,
432 M.V., Barrett, A., Burrows, C., Tarasov, A.I., et al. (2018). Electrophysiological properties of
433 human beta-cell lines EndoC- β H1 and - β H2 conform with human beta-cells. *Sci. Rep.* *8*,
434 16994. <https://doi.org/10.1038/s41598-018-34743-7>.
- 435 Hodson, D.J., Mitchell, R.K., Marselli, L., Pullen, T.J., Gimeno Brias, S., Semplici, F.,
436 Everett, K.L., Cooper, D.M.F., Bugliani, M., Marchetti, P., et al. (2014). ADCY5 Couples
437 Glucose to Insulin Secretion in Human Islets. *Diabetes* *63*, 3009–3021.
438 <https://doi.org/10.2337/db13-1607>.
- 439 Hughes, J.R., Roberts, N., McGowan, S., Hay, D., Giannoulatou, E., Lynch, M., De Gobbi,
440 M., Taylor, S., Gibbons, R., and Higgs, D.R. (2014). Analysis of hundreds of cis-regulatory
441 landscapes at high resolution in a single, high-throughput experiment. *Nat. Genet.* *46*, 205–
442 212. <https://doi.org/10.1038/ng.2871>.
- 443 Javierre, B.M., Burren, O.S., Wilder, S.P., Kreuzhuber, R., Hill, S.M., Sewitz, S., Cairns, J.,
444 Wingett, S.W., Várnai, C., Thiecke, M.J., et al. (2016). Lineage-Specific Genome
445 Architecture Links Enhancers and Non-coding Disease Variants to Target Gene Promoters.
446 *Cell* *167*, 1369-1384.e19. <https://doi.org/10.1016/j.cell.2016.09.037>.
- 447 Lawlor, N., Márquez, E.J., Orchard, P., Narisu, N., Shamim, M.S., Thibodeau, A., Varshney,
448 A., Kursawe, R., Erdos, M.R., Kanke, M., et al. (2019). Multiomic Profiling Identifies cis-
449 Regulatory Networks Underlying Human Pancreatic β Cell Identity and Function. *Cell Rep.*
450 *26*, 788-801.e6. <https://doi.org/10.1016/j.celrep.2018.12.083>.
- 451 Liao, Y., Smyth, G.K., and Shi, W. (2019). The R package Rsubread is easier, faster, cheaper
452 and better for alignment and quantification of RNA sequencing reads. *Nucleic Acids Res.* *47*,
453 e47–e47. <https://doi.org/10.1093/nar/gkz114>.
- 454 Love, M.I., Huber, W., and Anders, S. (2014). Moderated estimation of fold change and
455 dispersion for RNA-seq data with DESeq2. *Genome Biol.* *15*, 1–21.
456 <https://doi.org/10.1186/s13059-014-0550-8>.
- 457 Mahajan, A., Spracklen, C.N., Zhang, W., Ng, M.C.Y., Petty, L.E., Kitajima, H., Yu, G.Z.,
458 Rueger, S., Speidel, L., Kim, Y.J., et al. (2020). Trans-ancestry genetic study of type 2
459 diabetes highlights the power of diverse populations for discovery and translation. *MedRxiv*
460 2020.09.22.20198937-2020.09.22.20198937. <https://doi.org/10.1101/2020.09.22.20198937>.
- 461 Miguel-Escalada, I., Bonàs-Guarch, S., Cebola, I., Ponsa-Cobas, J., Mendieta-Esteban, J.,
462 Atla, G., Javierre, B.M., Rolando, D.M.Y., Farabella, I., Morgan, C.C., et al. (2019). Human
463 pancreatic islet three-dimensional chromatin architecture provides insights into the genetics
464 of type 2 diabetes. *Nat. Genet.* *51*, 1137–1148. <https://doi.org/10.1038/s41588-019-0457-0>.
- 465 Morris, A.P., Voight, B.F., Teslovich, T.M., Ferreira, T., Segrè, A.V., Steinthorsdottir, V.,
466 Strawbridge, R.J., Khan, H., Grallert, H., Mahajan, A., et al. (2012). Large-scale association

- 467 analysis provides insights into the genetic architecture and pathophysiology of type 2
468 diabetes. *Nat. Genet.* <https://doi.org/10.1038/ng.2383>.
- 469 Peiris, H., Park, S., Louis, S., Gu, X., Lam, J.Y., Asplund, O., Ippolito, G.C., Bottino, R.,
470 Groop, L., Tucker, H., et al. (2018). Discovering human diabetes-risk gene function with
471 genetics and physiological assays. *Nat. Commun.* *9*, 3855. [https://doi.org/10.1038/s41467-](https://doi.org/10.1038/s41467-018-06249-3)
472 [018-06249-3](https://doi.org/10.1038/s41467-018-06249-3).
- 473 Ravassard, P., Hazhouz, Y., Pechberty, S., Bricout-Neveu, E., Armanet, M., Czernichow, P.,
474 and Scharfmann, R. (2011). A genetically engineered human pancreatic β cell line exhibiting
475 glucose-inducible insulin secretion. *J. Clin. Invest.* *121*, 3589–3597.
476 <https://doi.org/10.1172/JCI58447>.
- 477 Su, C., Gao, L., May, C.L., Pippin, J.A., Boehm, K., Lee, M., Liu, C., Pahl, M.C., Golson,
478 M.L., Najj, A., et al. (2022). 3D chromatin maps of the human pancreas reveal lineage-
479 specific regulatory architecture of T2D risk. *Cell Metab.* *34*, 1394-1409.e4.
480 <https://doi.org/10.1016/j.cmet.2022.08.014>.
- 481 Telenius, J.M., Downes, D.J., Sergeant, M., Oudelaar, A.M., McGowan, S., Kerry, J.,
482 Hanssen, L.L.P., Schwessinger, R., Eijsbouts, C.Q., Davies, J.O.J., et al. (2020).
483 CaptureCompendium: a comprehensive toolkit for 3C analysis (Bioinformatics).
- 484 Thurner, M., van de Bunt, M., Torres, J.M., Mahajan, A., Nylander, V., Bennett, A.J.,
485 Gaulton, K.J., Barrett, A., Burrows, C., Bell, C.G., et al. (2018). Integration of human
486 pancreatic islet genomic data refines regulatory mechanisms at type 2 diabetes susceptibility
487 loci. *ELife* <https://doi.org/10.7554/eLife.31977>.
- 488 Viñuela, A., Varshney, A., van de Bunt, M., Prasad, R.B., Asplund, O., Bennett, A.,
489 Boehnke, M., Brown, A.A., Erdos, M.R., Fadista, J., et al. (2020). Genetic variant effects on
490 gene expression in human pancreatic islets and their implications for T2D. *Nat. Commun.* *11*,
491 4912–4912. <https://doi.org/10.1038/s41467-020-18581-8>.
- 492 Voight, B., Scott, L., Steinthorsdottir, V., Morris, A., Dina, C., Welch, R., Zeggini, E., Huth,
493 C., Aulchenko, Y., Thorleifsson, G., et al. (2010). Twelve type 2 diabetes susceptibility loci
494 identified through large-scale association analysis. *Nat. Genet.* *42*, 579–589. .
- 495 Wingett, S.W., Ewels, P., Furlan-Magaril, M., Nagano, T., Schoenfelder, S., Fraser, P., and
496 Andrews, S. (2015). HiCUP: pipeline for mapping and processing Hi-C data. *F1000Research*
497 *4*, 1310. <https://doi.org/10.12688/f1000research.7334.1>.
- 498
- 499

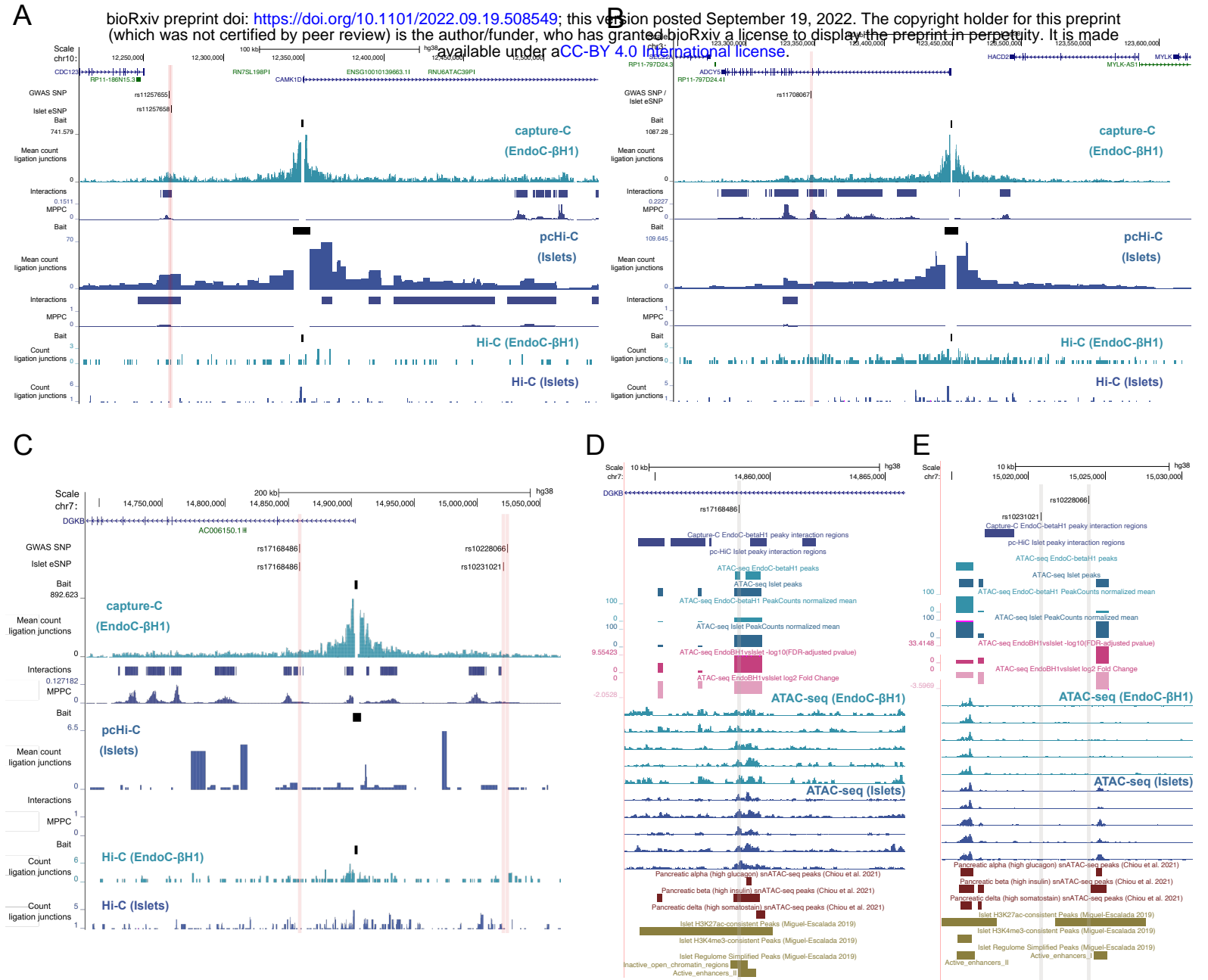


Figure 1.